

# Ivy-Fake: A Unified Explainable Framework and Benchmark for Image and Video AIGC Detection

Changjiang Jiang<sup>♣</sup>    Wenhui Dong<sup>♣,✉</sup>    Zhonghao Zhang    Chenyang Si  
Fengchang Yu    Wei Peng    Xinbin Yuan    Yifei Bi    Ming Zhao    Zian Zhou  
Caifeng Shan

$\pi^3$ Lab<sup>\*</sup>

## Abstract

*The rapid development of Artificial Intelligence Generated Content (AIGC) techniques has enabled the creation of high-quality synthetic content, but it also raises significant security concerns. Current detection methods face two major limitations: (1) the lack of multidimensional explainable datasets for generated images and videos. Existing open-source datasets (e.g., WildFake, GenVideo) rely on oversimplified binary annotations, which restrict the explainability and trustworthiness of trained detectors. (2) Prior MLLM-based forgery detectors (e.g., FakeVLM) exhibit insufficiently fine-grained interpretability in their step-by-step reasoning, which hinders reliable localization and explanation. To address these challenges, we introduce Ivy-Fake, the first large-scale multimodal benchmark for explainable AIGC detection. It consists of over 106K richly annotated training samples (images and videos) and 5,000 manually verified evaluation examples, sourced from multiple generative models and real-world datasets through a carefully designed pipeline to ensure both diversity and quality. Furthermore, we propose Ivy-xDetector, a reinforcement learning model based on Group Relative Policy Optimization (GRPO), capable of producing explainable reasoning chains and achieving robust performance across multiple synthetic content detection benchmarks. Extensive experiments demonstrate the superiority of our dataset and confirm the effectiveness of our approach. Notably, our method improves performance on GenImage from 86.88% to 96.32%, surpassing prior state-of-the-art methods by a clear margin.*

## 1. Introduction

The rapid development of diffusion-based models has triggered an exponential growth in Artificial Intelligence Generated Content (AIGC), like Sora [9], DALL-E [4], Imagen [40], and Stable Diffusion [38], which have redefined state-of-the-art performance in text-to-image synthesis. However, these advances also raise significant security concerns, including the misuse of DeepFake [35], document tampering [35], and dataset poisoning [42]. The increasing realism of synthetic content blurs the boundary between genuine and fabricated media, posing critical challenges for misinformation control, content provenance verification, and the preservation of public trust.

However, most existing approaches primarily focus on binary authenticity classification [2, 12, 23, 50], which limits the human interpretability of model predictions [54]. Existing benchmarks also remain inadequate for evaluating explainable AIGC detection. Datasets such as AIGCDetectionBenchmark [59] and GenVideo [12] provide only binary labels, while more recent resources like LOKI [54] attempt to incorporate fine-grained anomaly annotations across modalities but are still constrained in scale and diversity. On the other hand, current methods such as AIDE [50] and Demamba [12] are limited to a single modality—either image or video—without exploring unified detection across both domains. Similarly, existing datasets exhibit the same fragmentation: FakeBench [31] emphasizes explainable fake image detection but omits video content, whereas FakeClue [47] provides extensive image-level annotations yet lacks integrated video data. This fragmentation leads to substantial gaps in benchmarking and hinders unified advancement in explainable multimodal AIGC detection.

To address these challenges, we propose Ivy-Fake, a comprehensive dataset designed to evaluate explainable multimodal AIGC detection. Ivy-Fake offers: 1) Diverse Multimodal Data, a large-scale dataset comprising 61,107

<sup>0</sup>♣ Equal Contributions.

<sup>1</sup>✉Corresponding author: wenhui.dong@pi3lab.com.

<sup>2</sup>★ The complete author list is provided in the appendix.

<sup>3</sup>🔗 Code

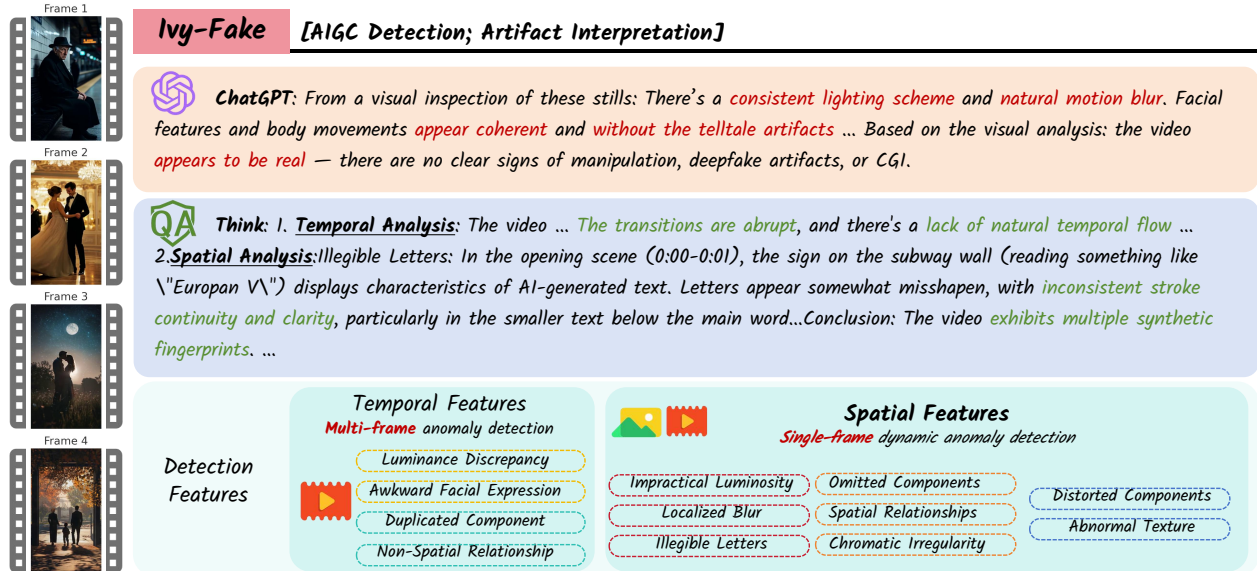


Figure 1. Overview of the Ivy-Fake framework: By conducting in-depth analysis of temporal and spatial artifacts, the framework enables explainable detection of AI-generated content.

annotated images and 45,272 annotated videos for training, along with 5,000 samples for evaluation. 2) Explainable Annotations, rich annotations that extend beyond binary labels to include detailed reasoning, enabling nuanced evaluation of models’ interpretability and explanatory capabilities.

In addition to providing Ivy-Fake, we introduce Ivy-xDetector, a model for detecting AI-generated images and videos and explaining the associated artifacts. As demonstrated by Figure 1, unlike other MLLMs, Ivy-xDetector excels at spotting generative artifacts, spatial in images and both spatial and temporal in videos. By integrating multiple spatial and temporal feature extractors, it detects image-level artifacts and video-level temporal inconsistencies with superior accuracy. Through the incorporation of explainable annotations and carefully curated domain-diverse data, our approach achieves state-of-the-art performance using only a fraction of the data required by existing detectors. While prior image/video classifiers [12, 50, 59] often rely on millions (M-level) of samples, our method attains superior performance across both image and video AIGC detection tasks with fewer than 200K samples.

Our main contributions are summarized as follows:

- We introduce Ivy-Fake, the first large-scale dataset for explainable AIGC detection across both images and videos, comprising 106,379 training samples and 5,000 manually verified test instances. Each entry is enriched with fine-grained visual annotations and textual reasoning to support transparent multimodal evaluation and future research.
- We propose Ivy-xDetector, a reinforcement learning-based model by Reinforcement Learning with Verifi-

able Rewards (RLVR) built upon GRPO, which achieves superior performance on multiple image and video detection benchmarks using fewer than 200K samples—significantly outperforming existing methods that rely on millions of data points.

- We conduct extensive experiments to validate the effectiveness of both the dataset and the model, demonstrating their substantial impact on improving multimodal large models’ capability in synthetic content detection.

## 2. Dataset

### 2.1. Data Collection

The Ivy-Fake dataset is curated from GenVideo [12], LOKI [54], FakeClue [47], WildFake [23], Kinetics-400 [25], and MMFakeBench [31]. Since Ivy-Fake is substantially larger than other datasets, we primarily detail our data processing procedures here.

**Image/Video Corruption Filtering.** The integrity of images and videos is critical for MLLM training. We observed that the official GenVideo [12] repository contained a large number of unreadable videos. To ensure data quality, we employed the official Qwen2.5-VL [3] I/O library to filter out corrupted files, discarding images and videos that failed to load.

**Image/Video Resolution.** To maintain consistency, we only retained images whose resolutions fell within [3,136, 12,845,056] pixels, and videos whose per-frame resolutions were within [100,352, 602,112] pixels, with the additional

constraint that total pixels did not exceed 19,267,968. Samples outside these ranges were discarded.

**Near-Duplicate Image Filtering.** Selecting challenging and diverse samples is crucial for model robustness. We extracted visual features from images and video frames using CLIP [36] and computed intra-class similarity scores. Images with excessively high similarity were removed, while videos were left unprocessed. To comprehensively activate and enhance the model’s reasoning capabilities across the task, we propose a high-quality data construction pipeline that integrates explainable detection of AI-generated content.

**Public Dataset Sources** The Ivy-Fake training set comprises approximately 106K image and video samples collected during the cold-start phase from diverse sources to ensure broad coverage of contemporary generative models. A significant portion was sourced from established public datasets, including GenVideo [12], LOKI [54], FakeClue [47], WildFake [23], Kinetics-400 [25], MM-FakeBench [31], GenImage [62], DiffusionForensics [46]. The cold-start phase aimed to enhance the granularity of interpretable content. To further improve the detector’s accuracy, an additional 87,500 image/video samples were stratified and sampled from multiple datasets for RLVR training, including MSRVT [49] (9,000 videos), GenImage [62] (32,000 images per category), CnnSpot [45] (19,000 samples), DigiFakeAV [30] (2,000 samples), GenVideo [12] (Fake subset) (9,000 samples), DiffusionForensics [46] (4,500 samples), WildFake [23] (12,000 samples), and synthetic data generated by Qwen-Image [48] (634 samples). In total, the dataset used for training comprises 194,513 samples.

**Generated Sources** To further enrich the dataset and better capture synthetic images prevalent in real-world scenarios, additional samples were generated using a diverse set of state-of-the-art image generation models. These models span multiple architectures and training paradigms, ensuring broad coverage of visual styles and generative patterns for robust evaluation. Specifically, extra sources include samples generated by FLUX.1 [27], Lora Flux [27] and Qwen-Image [48].

To ensure balanced representation across generative models and avoid potential biases, a stratified sampling strategy was employed during data collection. This approach maintained proportional inclusion of samples from each generator type, thereby preserving the diversity of visual content and facilitating fair and comprehensive evaluation across detection models.

## 2.2. Data Annotation

To generate explainable annotations, we employed the multimodal large language model Gemini 2.5 Pro [44], leveraging a knowledge distillation process to produce structured, interpretable outputs. To ensure consistent and structured output, we adapted the distillation template from DeepSeek-R1-Zero [19], which requires the model to first articulate a reasoning process before issuing a final determination.

To enhance annotation accuracy and guide the generation of relevant explanations, we incorporated category-level prior knowledge during annotation. Specifically, Gemini was provided with the ground truth authenticity label (i.e., "real" or "fake") and instructed to explain the rationale behind this classification. The user prompt was standardized as follows: This {file\_type} is {label}. Explain the reason. To further ensure the quality and consistency of explainable annotations, we conducted a comprehensive human alignment and verification process, as detailed in Appendix 10.

As illustrated in Table 1, `file_type` indicates the modality of the input—either "image" or "video"—and `{label}` represents the ground-truth label, assigned as either "real" or "fake". The distilled explanations were further categorized along two major dimensions to facilitate structured analysis: **Spatial Features**, which comprises eight sub-dimensions and captures artifacts and inconsistencies observable within individual frames or static images. **Temporal Features**, which includes four sub-dimensions and describes anomalies associated with motion, temporal coherence, and cross-frame consistency. Since still images inherently lack temporal attributes, this category is exclusively applicable to video annotations. These categories were informed by established taxonomies of visual artifacts in generative content, as detailed in prior research [15].

## 2.3. Comparison with Existing Datasets

A comparative overview of Ivy-Fake and several existing AIGC detection datasets is provided in Table 2. Notably, Ivy-Fake offers unique advantages by integrating explainable annotations across both image and video modalities, addressing a significant gap in current resources.

In contrast, datasets such as FakeClue [47] and FakeBench [31] provide only limited annotated samples, thereby restricting their applicability primarily to evaluation scenarios rather than serving as robust resources for model training. Similarly, LOKI [54], while offering explainability-focused annotations, is confined to a single modality (images) and evaluates across fewer dimensions. This constraint limits its suitability for comprehensive research on multimodal AIGC detection and explainability.

We identified a long-tail distribution in the distilled dataset, with a small portion of samples exhibiting token

Table 1. Task examples of Ivy-Fake.

Features	Sub Dimension	Example
Spatial	Impractical Luminosity	<i>Which visual clue reveals an impossible spatial or lighting configuration in the scene?</i> (A) Light direction opposite source. (B) Face without lighting. (C) Dark background, bright face. (D) Bright background, dark face.
	Localized Blur	<i>Which clue shows local blur or focus inconsistency?</i> (A) Clear face but blurred hand. (B) Sharp background, fuzzy hair. (C) Glasses edges blurred, eyes clear. (D) Hand blurred while holding clear object.
	Illegible Letters	<i>Which part of the document text is tampered or altered?</i> (A) Text blurred or half missing. (B) Letters inconsistent in size. (C) Words overlap or melt together. (D) Signs contain random symbols.
	Omitted Components	<i>Which part of the person looks incomplete or missing?</i> (A) Missing one finger. (B) Two fingers merged. (C) Missing eyebrows. (D) Three pairs of glasses.
	Spatial Relationships	<i>Where does the spatial relation look unnatural or physically impossible?</i> (A) Arm passes through body. (B) Legs overlap unnaturally. (C) Head detached from neck. (D) Hand holds object from wrong side.
	Distorted Components	<i>Which part appears deformed or stretched in shape?</i> (A) Finger bent at odd angle. (B) Eye stretched sideways. (C) Mouth warped or uneven. (D) Hand larger than face.
	Chromatic Irregularity	<i>Which clue shows unnatural or inconsistent colors in the image?</i> (A) Face partly blue under warm light. (B) Green reflection on red shirt. (C) Sky color bleeds into hair. (D) Background color unevenly saturated.
	Abnormal Texture	<i>What visual area shows abnormal or inconsistent texture?</i> (A) Skin looks like plastic. (B) Hair pattern repeats unnaturally. (C) Cloth surface too smooth or glossy. (D) Wall texture mixed with skin.
	Luminance Discrepancy	<i>Which moment shows sudden or inconsistent brightness between frames?</i> (A) Light flickers without reason. (B) Face turns dark while background stays bright. (C) Shadow jumps between frames. (D) Object brightness changes abruptly.
	Temporal	Awkward Facial Expression
Duplicated Component		<i>Where does an object or body part appear twice across frames?</i> (A) Two faces shown in one frame. (B) Hand shadow moves separately. (C) Extra arm appears then fades. (D) Same object duplicated in next frame.
Non-Spatial Relationships		<i>When does the action sequence look illogical or out of order?</i> (A) Person closes door before touching it. (B) Cup moves without contact. (C) Smile appears after laughter. (D) Object vanishes then reappears suddenly.

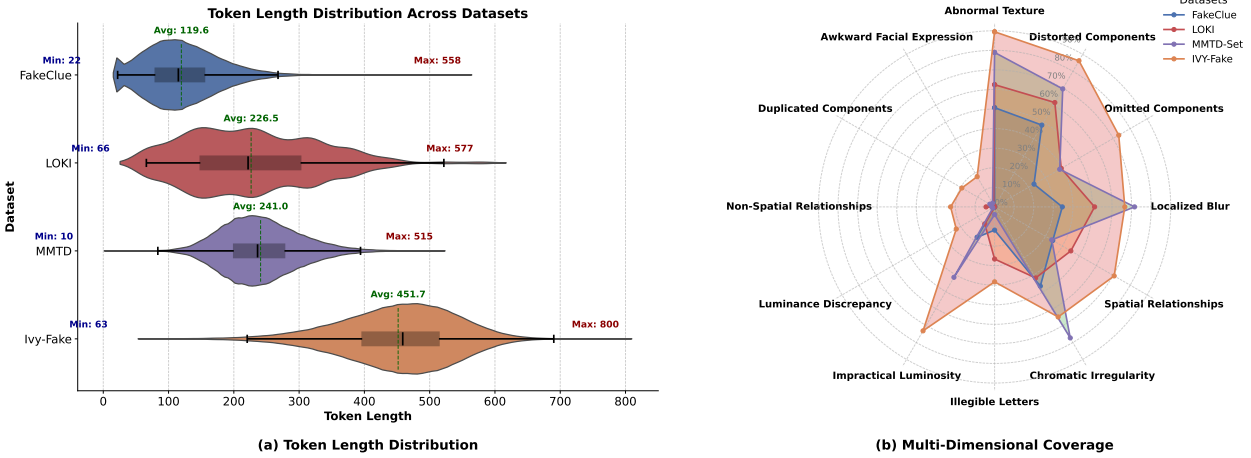


Figure 2. Token Length Distributions and Multi-Dimensional Coverage Across Datasets. Left: Distribution of token lengths across datasets; Right: Coverage of multiple dimensions in explainability datasets, extracted using Qwen3-32B [52]. The Prompt can be seen in appendix.

Table 2. Comparison on the different datasets used in binary classification and interpretability tasks. Token lengths are computed using the GPT-4o tokenizer from the tiktoken library.

Dataset	Avg Token Lengths	Generator	Modality	Dataset	
				fake	real
FakeBench [31]	-	6	Image	3K	3K
VANE-Bench [5]	101	5	Image*	2K	1K
LOKI [54]	226.5	~16	Image+Video	3K	0
FakeClue [47]	119.6	26	Image	68K	36K
Ivy-Fake	451.7	>30	Image+Video	53K	78K

lengths concentrated at both extremes. To mitigate the influence of these outliers, we retained only the central 90% of the distribution, filtering out the top and bottom 5% of samples, thereby keeping data with token lengths between 60

and 800. As shown in Figure 2 panel (a), Ivy-Fake exhibits the longest token length distribution, with an average token length of 451.7. Additionally, to conduct a fine-grained analysis of the semantic dimensions embedded in the explanatory language across different interpretability datasets, we employ Qwen3-32B [52] for dimension extraction. To enhance the accuracy of the extraction, we embed supplementary contextual information from each dataset into the model input. For example, in LOKI [54], the bounding box coordinates are wrapped with `<bbox>`/`</bbox>` tags, while metadata such as coordinates, titles, and fine-grained descriptions are also included as input to the model. Moreover, we set the Temperature to 0.8 and perform three extraction passes for each sample, retaining only the dimensions consistently identified across all runs. The final ag-

gregated results are visualized in panel (b).

As shown in Figure 3, Ivy-Fake outperforms FakeVLM in terms of interpretability. While FakeVLM only explains superficial factors such as lighting and texture, Ivy-Fake considers **multiple semantic dimensions**, including hair, skin, and background, leading to a more comprehensive understanding of forged content. The more image and video cases can be found in Appendix 15.

## 2.4. Quality Control

To mitigate the impact of hallucinations from Gemini 2.5 Pro during question generation, we sampled 8,000 cases for manual review. Each chain-of-thought (CoT) involving Gemini underwent at least two rounds of human verification. A total of ten users, including senior university students and regular participants, contributed to the verification process, which required approximately 1,000 hours in total. Each case was tested by at least two users to ensure robustness across different modalities of synthetic data. After this rigorous filtering, we retained 5,000 cases as the benchmark test set, consisting of 2,500 image samples and 2,500 video samples, with each modality containing 1,250 real and 1,250 fake instances. The complete dataset distribution is provided in Appendix 11.

## 3. Methodology

Our preliminary investigations revealed that existing MLLMs exhibit inadequate performance on these tasks. To overcome this limitation, we propose Ivy-xDetector, a multimodal large language model designed explicitly for robust and explainable AIGC detection. The overall training pipeline is illustrated in Figure 4.

**Stage 1: Cold Start for Instruction-Driven Detection and Explainability.** As shown in Figure 3, due to limited reasoning ability, existing models struggle to detect AIGC content and generate reliable explanations. To address this, we inject Gemini-generated detection and explanatory COT into the training process, thereby improving the model’s fine-grained artifact perception and explanation quality. This stage aims to initialize Ivy-xDetector with instruction-following and explainability capabilities. The resulting model not only performs accurate AIGC detection but also generates coherent, human-understandable rationales for its classifications.

**Stage 2: Sparse Rewards in Fine-grained Visual forgery Reasoning via Reinforcement Learning** Although the fine-tuned model from Stage 1 demonstrates improved artifact awareness and interpretability, its generalization ability remains limited. To further enhance the model’s capacity for producing consistent and human-understandable ex-

planations, we adopt the Group Relative Policy Optimization (GRPO) algorithm [41]. GRPO enables reinforcement learning using only binary classification samples, achieving efficient and data-light optimization. A detailed description of GRPO and the reward functions for Ivy-xDetector can be found in Appendix 9.

We construct binary real/fake pairs from multiple datasets, each containing both authentic and synthetic images and videos. As illustrated in Figure 3, Ivy-xDetector takes the visual input and extracts the text enclosed within the `<conclusion>... </conclusion>` tags, where the predicted label is either *real* or *fake*. The quantitative results of different training stages are presented in Table 7.

## 4. Experiments

### 4.1. Experimental Details

**Baselines** We primarily evaluate three closed-source models and three open-source models on our Ivy-Fake. The closed-source models are GPT-4o [1] and Gemini2.5 Flash [44]. For the open-source models, we select models of comparable size: InternVL3.5 [13], Qwen2.5-VL [3], MiMo-VL [43], LLaVA-OneVision-1.5 [14, 28] and MiniCPM-V-4.5 [53, 55]. Ivy-xDetector denotes our fully RL-trained model after the GRPO optimization stage.

**Evaluation** We report standard accuracy (Acc) and macro-averaged F1 score (F1) to assess the model’s ability to distinguish real from fake instances. For the reasoning task, we measure the similarity between the model’s reasoning process and the reference annotations using the ROUGE-L score [29] and BertScore [20, 57], which captures the longest common subsequence between predicted and reference texts, reflecting token-level overlap. Since ROUGE-L may fail to fully capture the fidelity of reasoning steps, we adopt an LLM-as-a-judge evaluation paradigm [58], following the FakeBench protocol [31], which assesses model responses along four dimensions: (1) Completeness: It reflects the extent to which the response fully addresses all aspects of the user’s question. More complete responses should incorporate information aligning well with the “golden clues” or reference answers. Incomplete or partially answered responses will receive lower scores. (2) Relevance: Measure how closely the content relates to the original annotation; (3) Level of Detail: Assess whether the response includes enough examples or elaborations; (4) Explanation: Verify the accuracy and consistency of explanations for any causes mentioned. Each response is scored using GPT-4o mini [1] under a unified evaluation prompt (see Appendix 13), which instructs the model to act as an impartial judge and assign a score from 1 to 5.

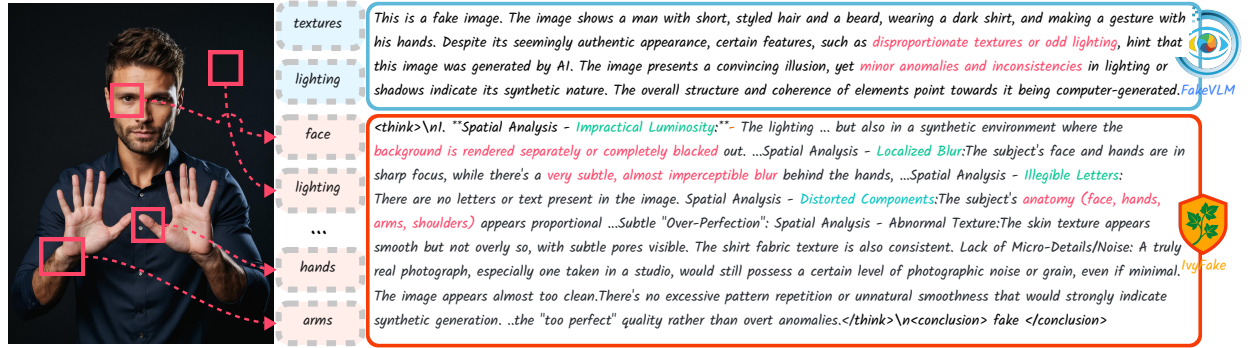


Figure 3. Comparison between Ivy-Fake and FakeVLM [47] (NeurIPS 2025). The Ivy-Fake dataset provides richer and more fine-grained interpretability dimensions.

Table 3. Performance comparison of models on image and video tasks. “Auto Metrics” include Acc, F1. “GPT Assisted” includes four subjective criteria: Comprehensiveness, Relevance, Detail, and Explanation. **Bold** indicates the best result, and underline indicates the second best.

Model	Image		Video		Overall	
	Auto Metrics	GPT Assisted	Auto Metrics	GPT Assisted	Auto Metrics	GPT Assisted
	Acc/F1/ROUGE-L/SIM	Com./Rel./Det./Exp.	Acc/F1/ROUGE-L/SIM	Com./Rel./Det./Exp.	Acc/F1/ROUGE-L/SIM	Com./Rel./Det./Exp.
<i>Closed-source MLLMs</i>						
GPT-4o	0.725/0.723/0.108/0.525	2.34/3.20/2.04/3.26	0.448/0.579/0.072/0.451	1.79/2.35/1.67/2.40	0.587/0.663/0.090/0.488	2.07/2.78/1.85/2.83
Gemini-2.5-Flash	<u>0.747/0.737/0.263/0.733</u>	<b>3.94/4.11/4.04/4.09</b>	<u>0.810/0.811/0.246/0.723</u>	<b>4.00/4.37/4.03/4.36</b>	<u>0.779/0.776/0.254/0.728</u>	<b>3.97/4.24/4.04/4.22</b>
<i>Open-source MLLMs</i>						
<i>7B-Parameters Models</i>						
InternVL3.5-8B	0.605/0.602/0.194/0.680	2.83/3.49/2.69/3.32	0.574/0.588/0.188/0.664	2.75/3.35/2.68/3.28	0.589/0.596/0.191/0.672	2.79/3.42/2.69/3.30
MiMo-VL-7B	0.662/0.637/0.121/0.593	1.99/2.80/1.85/2.89	0.778/0.783/0.112/0.580	2.04/2.91/1.90/3.19	0.720/0.715/0.116/0.586	2.01/2.86/1.87/3.04
Qwen2.5-VL-7B	0.013/0.026/0.006/0.264	1.02/1.03/1.01/1.52	0.092/0.159/0.015/0.280	1.14/1.23/1.12/2.21	0.053/0.096/0.010/0.272	1.08/1.13/1.07/1.86
LLaVA-OneVision-1.5-8B	0.500/0.333/0.080/0.499	1.51/2.62/1.49/2.38	0.500/0.333/0.068/0.481	1.49/2.26/1.37/2.19	0.500/0.333/0.074/0.490	1.50/2.44/1.43/2.28
MiniCPM-V-4.5	0.666/0.680/0.169/0.637	3.20/3.93/3.06/3.60	0.491/0.505/0.152/0.627	2.83/3.66/2.76/3.36	0.579/0.610/0.161/0.632	3.01/3.80/2.91/3.48
<i>3B-Parameters Models</i>						
Qwen2.5-VL-3B	0.641/0.612/0.023/0.391	1.19/1.33/1.18/3.28	0.689/0.686/0.017/0.381	1.42/1.56/1.40/3.68	0.665/0.652/0.020/0.386	1.31/1.45/1.29/3.48
Gemma-3-4b-it	0.408/0.477/0.170/0.576	2.55/3.36/2.46/3.11	0.396/0.482/0.149/0.561	2.30/3.03/2.37/2.95	0.402/0.482/0.159/0.568	2.43/3.19/2.42/3.03
InternVL3.5-2B	0.602/0.573/0.177/0.648	2.62/3.29/2.51/3.13	0.435/0.459/0.159/0.631	2.46/3.16/2.42/2.99	0.518/0.518/0.168/0.640	2.54/3.22/2.47/3.06
InternVL3.5-4B	0.651/0.652/0.190/0.660	3.01/3.68/2.95/3.58	0.614/0.617/0.181/0.653	2.93/3.61/2.83/3.52	0.632/0.635/0.186/0.656	2.97/3.64/2.89/3.55
Ivy-xDetector	<b>0.831/0.831/0.283/0.714</b>	<u>3.54/4.04/3.61/3.85</u>	<b>0.897/0.897/0.300/0.726</b>	<u>3.72/4.12/3.75/4.24</u>	<b>0.864/0.864/0.291/0.720</b>	<u>3.63/4.08/3.68/4.05</u>

**Implementation Details** Our model was trained using the AdamW [32] optimizer with a cosine learning rate schedule. During the SFT stage, the model was trained for one epoch with a batch size of 1, which ensures stable convergence on large-scale multimodal data. In the subsequent RL stage, we adopted the GRPO algorithm, training for one epoch with the same batch size and a learning rate of  $1 \times 10^{-5}$ . Within GRPO, the group size  $n$  was set to 8, the warm-up ratio to 0.01, the temperature to 0.9. Training the SFT and RL stages required approximately 10 and 50 hours, respectively, on a system equipped with 32 A100 GPUs.

For video-based inputs, we configured the preprocessing pipeline to sample frames at a rate of 1 frame per sec-

ond, with a maximum of 6 frames per clip to ensure temporal coherence while maintaining computational efficiency. Across the training pipeline, the overall input resolution was constrained by a global upper bound of 6,422,528 pixels (MAX\_PIXELS), preventing overflow during multi-GPU parallel training and ensuring consistent input scaling across image and video modalities.

## 4.2. Main Results

We perform extensive experiments to assess both detection and explanation capabilities. In particular, the proposed method is evaluated on the classification (real/fake) tasks and reasoning tasks for both image and video content using

Table 4. Comparison on the **Chameleon** [50]. Accuracy (%) of different detectors (rows) in detecting real and fake images. For each training dataset, the first row is overall accuracy, the second row is “fake/real” class accuracy.

CNNSpot	FreDect	Fusing	GramNet	LNP	UnivFD	DIRE	PatchCraft	NPR	AIDE	Ivy-xDetector
60.89	57.22	57.09	60.95	58.52	60.42	59.71	56.32	58.13	65.77	<b>73.17</b>
9.86/99.25	0.89/99.55	0.02/99.98	4.76/99.66	7.72/96.70	85.52/41.56	11.86/95.67	3.07/96.35	2.43/100.00	26.80/95.06	67.78/77.22

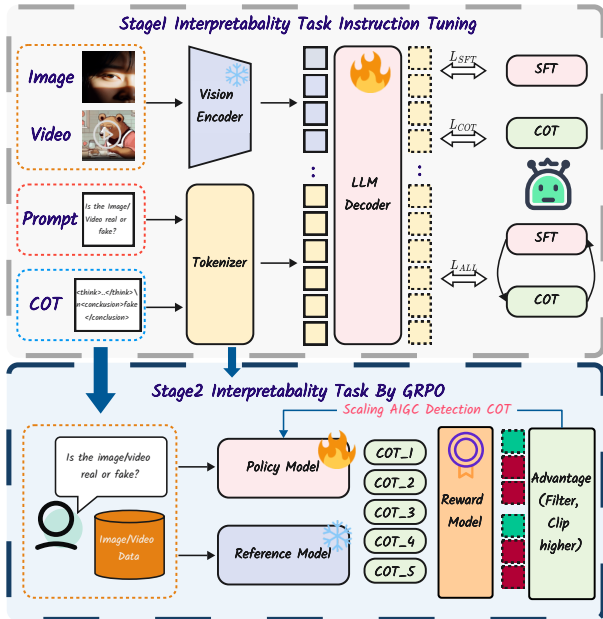


Figure 4. Overview of the three-stage training pipeline for Ivy-xDetector, including general video understanding, detection instruction tuning, and interpretability instruction tuning.

Table 5. Comparison on the **Genimage** [62]. Accuracy (%) of different detectors (rows) in detecting real and fake images from different generators (columns). The best result and the second-best result are marked in bold and underline, respectively. Results of other methods are reported from [50].

Method	Midjourney	SD v1.4	SD v1.5	ADM	GLIDE	Wukong	VQDM	BigGAN	Mean
CNNSpot [45]	52.80	96.30	95.90	50.10	39.80	78.60	53.40	46.80	64.21
F3Net [34]	50.10	<b>99.90</b>	<b>99.90</b>	49.90	50.00	<b>99.90</b>	49.90	49.90	68.69
DIRE [46]	60.20	<b>99.90</b>	<b>99.80</b>	50.90	55.00	99.20	50.10	50.20	70.66
GenDet [61]	89.60	96.10	96.10	58.00	78.40	92.80	66.50	75.00	81.56
PatchCraft [59]	79.00	89.50	89.30	77.30	78.40	89.30	83.70	72.40	82.30
FRIDA [7]	85.80	85.00	85.50	84.00	87.30	83.90	86.50	84.80	85.30
AIDE [50]	79.38	<u>99.74</u>	99.76	78.54	91.82	98.65	80.26	66.89	86.88
DRCT [11]	91.50	95.00	94.40	<u>79.40</u>	89.20	94.70	90.00	81.70	89.50
Effort [51]	82.40	99.80	99.80	78.70	<u>93.30</u>	97.40	<u>91.70</u>	<u>77.60</u>	<u>91.10</u>
ThinkFake-7B [24]	<u>92.50</u>	93.10	95.30	73.10	87.40	93.60	66.20	70.80	84.00
Ivy-xDetector	<b>96.41</b>	97.07	97.14	<b>95.59</b>	<b>95.95</b>	96.92	<b>96.03</b>	<b>95.22</b>	<b>96.32</b>

the proposed unified framework. For the classification task, we test our model on both image and video content to detect the synthetic content.

From Table 3, our method demonstrates robust detection and explanation capabilities across both image and video tasks. Overall, closed-source models maintain a clear advantage in classification accuracy and subjective explanation quality. Among them, Gemini-2.5-flash achieves

Table 6. Comparisons to the **GenVideo** [12]. F1 score (F1), recall score (R) and average precision (AP) on the many-to-many generalization task. “Demamba-XCLIP-FT” is abbreviated as “Demamba”. Results of other methods are reported from [12].

Model	Metric	Sora	Morph Studio	Gen2	HotShot	Lavie	Show-1	Moon Valley	Crafter	Model Scope	Wild Scrape	Avg.
F3Net (Image)	R	0.8393	0.9971	0.9862	0.7757	0.5700	0.3657	0.9952	0.9971	0.8943	0.7678	0.8188
	F1	0.5900	0.9406	0.9628	0.8169	0.6988	0.4904	0.9332	0.9688	0.8573	0.8251	0.8024
NPR (Image)	R	0.9107	0.9957	0.9949	0.2429	0.8964	0.5771	0.9712	0.9986	0.9429	0.8780	0.8408
	F1	0.2786	0.8441	0.9131	0.3028	0.8627	0.5944	0.8170	0.9164	0.8184	0.8163	0.7164
STIL (Video)	R	0.7857	0.9814	0.9804	0.7600	0.6179	0.5329	0.8936	0.9736	0.9457	0.6501	0.8222
	F1	0.3805	0.9068	0.9458	0.7824	0.7232	0.6217	0.9039	0.9433	0.8884	0.7267	0.7823
DeMamba (Video)	R	0.9812	1.0000	0.9986	0.6543	0.9486	0.9886	1.0000	1.0000	0.9286	0.8909	0.9302
	F1	0.6407	0.9602	0.9790	0.7539	0.9537	0.9551	0.9537	0.9797	0.9240	0.9120	0.9020
Ivy-xDetector	R	0.7857	0.9371	0.9507	0.9443	0.9550	0.9643	0.9968	0.9857	0.8943	0.9461	0.9528
	F1	0.8800	0.9676	0.9747	0.9713	0.9770	0.9818	0.9984	0.9928	0.9442	0.9723	0.9526

the best performance on both automatic metrics and GPT-assisted evaluation (e.g., reaching Acc/F1 of 0.812/0.812 on video detection and an average explanation score above 4.0), reflecting strong overall detection and reasoning ability. In contrast, GPT-4o maintains relatively high classification accuracy.

For open-source models, most models in the 3B–7B parameter range exhibit relatively low scores on explanation dimensions (< 3.5), indicating limitations in generating reasoning chains and covering multi-dimensional details. Notably, Qwen2.5-VL-3B shows relatively stable performance in explanation relevance and detail (Det./Exp. > 3.2), suggesting that lightweight models still hold potential under specific designs.

Notably, Gemini-2.5-Flash achieves the highest scores across all explanation-related dimensions, with an average of 4.12, surpassing all other models. This advantage can be attributed to the fact that part of our training data was distilled from Gemini-2.5-Pro, a powerful multimodal model capable of handling complex reasoning and explanation tasks. In contrast, our Ivy-xDetector ranks second with an average explanation score of 3.85, demonstrating interpretability comparable to Gemini-2.5-Flash while achieving substantially higher detection accuracy (Acc/F1 = 0.864/0.864) than any other open-source model. Compared with Gemini-2.5-Flash (Acc/F1 = 0.780/0.776), Ivy-xDetector improves accuracy by over 10 percentage points, confirming its robustness in both synthetic image detection and interpretive reasoning tasks.

### 4.3. Generalization Evaluation

**Evaluation on Classification Benchmarks.** We conduct evaluations across multiple public leaderboards, including the image-based GenImage 5 and the video-based Gen-

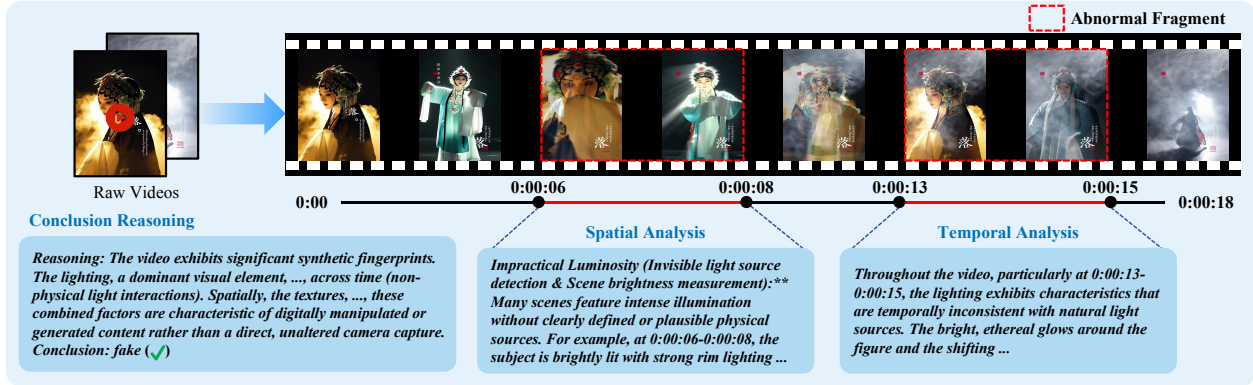


Figure 5. Ivy-xDetector performance on video detection. The model provides fine-grained spatiotemporal reasoning chains for explainable analysis.

Table 7. Ablation study on different SFT and RL training settings. *Base Model* denotes the base model Qwen2.5-VL-3B. Evaluation metric: ACC / F1.

Model Name	Training Stage SFT	RL	Chameleon (Image)	GenVideo (Video)	Ivy-Fake Test
Base Model			59.05 / 53.30	67.70 / 80.74	65.10 / 61.80
-	✓		40.31 / 37.99	91.61 / 91.55	73.91 / 73.83
-		✓	72.72 / 70.79	78.19 / 77.62	77.00 / 76.66
-	✓	✓	73.17 / 73.14	95.29 / 95.29	86.40 / 86.30

Video benchmark 6. Performance results of other competing detectors are taken from AIDE [50] and Demamba [12]. Our method achieves superior performance on all these leaderboards, demonstrating superior detection accuracy and robust cross-modal consistency.

**Evaluation on Unseen Benchmarks.** Beyond the datasets aligned with our training sets, we further evaluate the generalization ability of Ivy-xDetector on the Chameleon benchmark[50], which lies outside the training data distribution, as shown in Table 4. The results confirm that our approach preserves strong generalization capability across unseen generative models and diverse data domains.

Compared to the original leaderboard SOTA method **AIDE**, our model achieves an overall accuracy of **73.17%**. Notably, while the accuracy for the *real* class decreases from 95.06% to 77.22%, the accuracy for the *fake* class substantially increases from 26.80% to 67.78%. This suggests that **AIDE** tends to overfit the real category, whereas our model achieves a more balanced and robust performance across both real and synthetic content.

**Ablation Study.** To validate the effectiveness of our training framework, we design four ablation variants, as shown in Table 7. As shown, applying SFT alone results in only a slight performance drop on the out-of-domain benchmark Chameleon, while achieving consistent improvements

across all other datasets. This suggests that the SFT stage primarily enhances the model’s fine-grained sensitivity to synthetic artifacts. In contrast, applying RL alone yields modest but consistent gains in classification accuracy across benchmarks. The combination of SFT and RL achieves the best balance between accuracy and interpretability.

#### 4.4. Case Study

As illustrated in Figure 5, Ivy-xDetector demonstrates a rich single frame / video understanding across multiple dimensions, effectively capturing subtle differences in generated content. To further highlight its advantages over other models, we provide additional comparison cases with GPT-4o, Gemini-2.5, InternVL3, and Qwen2.5-VL in Appendix 15.

### 5. Conclusion

We introduced Ivy-Fake, the first unified, large-scale dataset for explainable AIGC detection across both images and videos, featuring over 131K richly annotated training samples and 5,000 evaluation examples with natural-language reasoning, and proposed Ivy Explainable Detector (Ivy-xDetector), a MLLM that jointly detects and explains synthetic content. Our model sets superior benchmarks in AIGC detection and explainability, and our publicly released resources provide a robust foundation for transparent, trustworthy multimodal analysis. We believe that such fine-grained explainability data Ivy-Fake can catalyze new research directions for the AIGC detection community, enabling deeper understanding of synthetic content and more principled model development.

**Limitations:** Future work will concentrate on tailoring the benchmark toward domain-specific scenarios, including explainability-focused datasets for DeepFake and document manipulation analysis. Nevertheless, our experiments suggest that the proposed approach exhibits strong scalability and generalization capabilities, indicating the potential for

even better performance when applied to larger models such as 32B or 72B.

**Broader impacts:** The data and model can be helped with the detection of fake visual content, help to uncover fact. Potentially, this can also be used to train stronger generative model to synthesize more realistic visual content.

## References

- [1] Josh Achiam, Steven Adler, Sandhini Agarwal, Lama Ahmad, Ilge Akkaya, Florencia Leoni Aleman, Diogo Almeida, Janko Altenschmidt, Sam Altman, Shyamal Anadkat, et al. Gpt-4 technical report. *arXiv preprint arXiv:2303.08774*, 2023. 5
- [2] Jianfa Bai, Man Lin, Gang Cao, and Zijie Lou. Ai-generated video detection via spatial-temporal anomaly learning. In *Chinese Conference on Pattern Recognition and Computer Vision (PRCV)*, pages 460–470. Springer, 2024. 1
- [3] Shuai Bai, Keqin Chen, Xuejing Liu, Jialin Wang, Wenbin Ge, Sibao Song, Kai Dang, Peng Wang, Shijie Wang, Jun Tang, et al. Qwen2.5-vl technical report. *arXiv preprint arXiv:2502.13923*, 2025. 2, 5
- [4] James Betker, Gabriel Goh, Li Jing, Tim Brooks, Jianfeng Wang, Linjie Li, Long Ouyang, Juntang Zhuang, Joyce Lee, Yufei Guo, et al. Improving image generation with better captions. *Computer Science*, 2(3):8, 2023. 1
- [5] Rohit Bharadwaj, Hanan Gani, Muzammal Naseer, Fahad Shahbaz Khan, and Salman Khan. Vane-bench: Video anomaly evaluation benchmark for conversational llms, 2024. 4
- [6] Andreas Blattmann, Tim Dockhorn, Sumith Kulal, Daniel Mendelevitch, Maciej Kilian, Dominik Lorenz, Yam Levi, Zion English, Vikram Voleti, Adam Letts, et al. Stable video diffusion: Scaling latent video diffusion models to large datasets. *arXiv preprint arXiv:2311.15127*, 2023. 1
- [7] Simone Bonechi, Paolo Andreini, and Barbara Toniella Corradini. Who made this? fake detection and source attribution with diffusion features, 2025. 7
- [8] Andrew Brock, Jeff Donahue, and Karen Simonyan. Large scale gan training for high fidelity natural image synthesis. *arXiv preprint arXiv:1809.11096*, 2018. 1
- [9] Tim Brooks, Bill Peebles, Connor Holmes, Will DePue, Yufei Guo, Li Jing, David Schnurr, Joe Taylor, Troy Luhman, Eric Luhman, Clarence Ng, Ricky Wang, and Aditya Ramesh. Video generation models as world simulators. *arXiv preprint arXiv:2405.19707*, 2024. 1
- [10] Bin Cao, Jianhao Yuan, Yexin Liu, Jian Li, Shuyang Sun, Jing Liu, and Bo Zhao. Synartifact: Classifying and alleviating artifacts in synthetic images via vision-language model. *arXiv preprint arXiv:2402.18068*, 2024. 1
- [11] Baoying Chen, Jishen Zeng, Jianquan Yang, and Rui Yang. Drct: diffusion reconstruction contrastive training towards universal detection of diffusion generated images. In *ICML. JMLR.org*, 2024. 7
- [12] Haoxing Chen, Yan Hong, Zizheng Huang, Zhuoer Xu, Zhangxuan Gu, Yaohui Li, Jun Lan, Huijia Zhu, Jianfu Zhang, Weiqiang Wang, and Huaxiong Li. Demamba: Ai-generated video detection on million-scale genvideo benchmark. *arXiv preprint arXiv:2405.19707*, 2024. 1, 2, 3, 7, 8
- [13] Zhe Chen, Jiannan Wu, Wenhai Wang, Weijie Su, Guo Chen, Sen Xing, Muyan Zhong, Qinglong Zhang, Xizhou Zhu, Lewei Lu, et al. Internvl: Scaling up vision foundation models and aligning for generic visual-linguistic tasks. In *Proceedings of the IEEE/CVF Conference on Computer Vision and Pattern Recognition*, pages 24185–24198, 2024. 5
- [14] LLaVA Community Contributors. Llava-onevision-1.5: Fully open framework for democratized multimodal training. In *arxiv*, 2025. 5
- [15] Jingyi Deng, Chenhao Lin, Zhengyu Zhao, Shuai Liu, Qian Wang, and Chao Shen. A survey of defenses against ai-generated visual media: Detection, disruption, and authentication. *arXiv preprint arXiv:2407.10575*, 2024. 3, 1
- [16] Prafulla Dhariwal and Alexander Nichol. Diffusion models beat gans on image synthesis. *Advances in neural information processing systems*, 34:8780–8794, 2021. 1
- [17] Shichao Dong, Jin Wang, Jiajun Liang, Haoqiang Fan, and Renhe Ji. Explaining deepfake detection by analysing image matching. In *European conference on computer vision*, pages 18–35. Springer, 2022. 1
- [18] Ian J Goodfellow, Jean Pouget-Abadie, Mehdi Mirza, Bing Xu, David Warde-Farley, Sherjil Ozair, Aaron Courville, and Yoshua Bengio. Generative adversarial nets. *Advances in neural information processing systems*, 27, 2014. 1
- [19] Daya Guo, Dejian Yang, Haowei Zhang, Junxiao Song, Ruoyu Zhang, Runxin Xu, Qihao Zhu, Shirong Ma, Peiyi Wang, Xiao Bi, et al. Deepseek-r1: Incentivizing reasoning capability in llms via reinforcement learning. *arXiv preprint arXiv:2501.12948*, 2025. 3, 2
- [20] Pengcheng He, Xiaodong Liu, Jianfeng Gao, and Weizhu Chen. Deberta: Decoding-enhanced bert with disentangled attention. In *International Conference on Learning Representations*, 2021. 5
- [21] Amir Hertz, Ron Mokady, Jay Tenenbaum, Kfir Aberman, Yael Pritch, and Daniel Cohen-Or. Prompt-to-prompt image editing with cross attention control. *arXiv preprint arXiv:2208.01626*, 2022. 1
- [22] Jonathan Ho, Ajay Jain, and Pieter Abbeel. Denoising diffusion probabilistic models. *Advances in neural information processing systems*, 33:6840–6851, 2020. 1
- [23] Yan Hong, Jianming Feng, Haoxing Chen, Jun Lan, Huijia Zhu, Weiqiang Wang, and Jianfu Zhang. Wildfake: A large-scale and hierarchical dataset for ai-generated images detection. *Proceedings of the AAAI Conference on Artificial Intelligence*, 39(4):3500–3508, 2025. 1, 2, 3
- [24] Tai-Ming Huang, Wei-Tung Lin, Kai-Lung Hua, Wen-Huang Cheng, Junichi Yamagishi, and Jun-Cheng Chen. Thinkfake: Reasoning in multimodal large language models for ai-generated image detection, 2025. 7
- [25] Will Kay, Joao Carreira, Karen Simonyan, Brian Zhang, Chloe Hillier, Sudheendra Vijayanarasimhan, Fabio Viola, Tim Green, Trevor Back, Paul Natsev, Mustafa Suleyman, and Andrew Zisserman. The kinetics human action video dataset, 2017. 2, 3

- [26] Mamadou Keita, Wassim Hamidouche, Hessen Bouguessa Eutamene, Abdelmalik Taleb-Ahmed, David Camacho, and Abdenour Hadid. Bi-lora: A vision-language approach for synthetic image detection. *Expert Systems*, 42(2):e13829, 2025. 1
- [27] Black Forest Labs, Stephen Batifol, Andreas Blattmann, Frederic Boesel, Saksham Consul, Cyril Diagne, Tim Dockhorn, Jack English, Zion English, Patrick Esser, Sumith Kulal, Kyle Lacey, Yam Levi, Cheng Li, Dominik Lorenz, Jonas Müller, Dustin Podell, Robin Rombach, Harry Saini, Axel Sauer, and Luke Smith. Flux.1 kontext: Flow matching for in-context image generation and editing in latent space, 2025. 3, 1
- [28] Bo Li, Yuanhan Zhang, Dong Guo, Renrui Zhang, Feng Li, Hao Zhang, Kaichen Zhang, Peiyuan Zhang, Yanwei Li, Ziwei Liu, and Chunyuan Li. Llava-onevision: Easy visual task transfer. *Transactions on Machine Learning Research*, 2024. 5
- [29] Chin-Yew Lin. Rouge: A package for automatic evaluation of summaries. In *Text summarization branches out*, pages 74–81, 2004. 5
- [30] Jiaxin Liu, Jia Wang, Saihui Hou, Min Ren, Huijia Wu, Long Ma, Renwang Pei, and Zhaofeng He. Beyond face swapping: A diffusion-based digital human benchmark for multimodal deepfake detection, 2025. 3
- [31] Xuannan Liu, Zekun Li, Peipei Li, Huaibo Huang, Shuhan Xia, Xing Cui, Linzhi Huang, Weihong Deng, and Zhaofeng He. Mmfakebench: A mixed-source multimodal misinformation detection benchmark for lvlms. In *ICLR*, 2025. 1, 2, 3, 4, 5
- [32] Ilya Loshchilov and Frank Hutter. Fixing weight decay regularization in adam. *ArXiv*, abs/1711.05101, 2017. 6
- [33] Alex Nichol, Prafulla Dhariwal, Aditya Ramesh, Pranav Shyam, Pamela Mishkin, Bob McGrew, Ilya Sutskever, and Mark Chen. Glide: Towards photorealistic image generation and editing with text-guided diffusion models. *arXiv preprint arXiv:2112.10741*, 2021. 1
- [34] Yuyang Qian, Guojun Yin, Lu Sheng, Zixuan Chen, and Jing Shao. Thinking in frequency: Face forgery detection by mining frequency-aware clues. In *European conference on computer vision*, pages 86–103. Springer, 2020. 7, 2
- [35] Shavez Mushtaq Qureshi, Atif Saeed, Sultan H. Almotiri, Farooq Ahmad, and Mohammed A. Al Ghamdi. Deepfake forensics: a survey of digital forensic methods for multimodal deepfake identification on social media. *PeerJ Computer Science*, 10, 2024. 1
- [36] Alec Radford, Jong Wook Kim, Chris Hallacy, Aditya Ramesh, Gabriel Goh, Sandhini Agarwal, Girish Sastry, Amanda Askell, Pamela Mishkin, Jack Clark, Gretchen Krueger, and Ilya Sutskever. Learning transferable visual models from natural language supervision. In *International Conference on Machine Learning*, 2021. 3
- [37] Robin Rombach, Andreas Blattmann, Dominik Lorenz, Patrick Esser, and Björn Ommer. High-resolution image synthesis with latent diffusion models. In *Proceedings of the IEEE/CVF conference on computer vision and pattern recognition*, pages 10684–10695, 2022. 1
- [38] Robin Rombach, Andreas Blattmann, Dominik Lorenz, Patrick Esser, and Björn Ommer. High-resolution image synthesis with latent diffusion models. In *Proceedings of the IEEE/CVF conference on computer vision and pattern recognition*, pages 10684–10695, 2022. 1
- [39] Olga Russakovsky, Jia Deng, Hao Su, Jonathan Krause, Sanjeev Satheesh, Sean Ma, Zhiheng Huang, Andrej Karpathy, Aditya Khosla, Michael Bernstein, Alexander C. Berg, and Li Fei-Fei. ImageNet Large Scale Visual Recognition Challenge. *International Journal of Computer Vision (IJCV)*, 115(3):211–252, 2015. 1
- [40] Chitwan Saharia, William Chan, Saurabh Saxena, Lala Li, Jay Whang, Emily L Denton, Kamyar Ghasemipour, Raphael Gontijo Lopes, Burcu Karagol Ayan, Tim Salimans, et al. Photorealistic text-to-image diffusion models with deep language understanding. *Advances in neural information processing systems*, 35:36479–36494, 2022. 1
- [41] Zhihong Shao, Peiyi Wang, Qihao Zhu, Runxin Xu, Junxiao Song, Xiao Bi, Haowei Zhang, Mingchuan Zhang, Y. K. Li, Y. Wu, and Daya Guo. Deepseekmath: Pushing the limits of mathematical reasoning in open language models, 2024. 5, 2
- [42] Jacob Steinhardt, Pang Wei Koh, and Percy Liang. Certified defenses for data poisoning attacks. In *Proceedings of the 31st International Conference on Neural Information Processing Systems*, page 3520–3532, Red Hook, NY, USA, 2017. Curran Associates Inc. 1
- [43] Core Team, Zihao Yue, Zhenru Lin, Yifan Song, Weikun Wang, Shuhuai Ren, Shuhao Gu, Shicheng Li, Peidian Li, Liang Zhao, Lei Li, Kainan Bao, Hao Tian, Hailin Zhang, Gang Wang, Dawei Zhu, Cici, Chenhong He, Bowen Ye, Bowen Shen, Zihan Zhang, Zihan Jiang, Zhixian Zheng, Zhichao Song, Zhenbo Luo, Yue Yu, Yudong Wang, Yuanyuan Tian, Yu Tu, Yihan Yan, Yi Huang, Xu Wang, Xinzhe Xu, Xingchen Song, Xing Zhang, Xing Yong, Xin Zhang, Xiangwei Deng, Wenyu Yang, Wenhan Ma, Weiwei Lv, Weiji Zhuang, Wei Liu, Sirui Deng, Shuo Liu, Shimao Chen, Shihua Yu, Shaohui Liu, Shande Wang, Rui Ma, Qiantong Wang, Peng Wang, Nuo Chen, Menghang Zhu, Kangyang Zhou, Kang Zhou, Kai Fang, Jun Shi, Jinhao Dong, Jiebao Xiao, Jiaming Xu, Huaqiu Liu, Hongshen Xu, Heng Qu, Haochen Zhao, Hanglong Lv, Guoan Wang, Duo Zhang, Dong Zhang, Di Zhang, Chong Ma, Chang Liu, Can Cai, and Bingquan Xia. Mimo-vl technical report, 2025. 5
- [44] Gemini Team, Rohan Anil, Sebastian Borgeaud, Jean-Baptiste Alayrac, Jiahui Yu, Radu Soricut, Johan Schalkwyk, Andrew M Dai, Anja Hauth, Katie Millican, et al. Gemini: a family of highly capable multimodal models. *arXiv preprint arXiv:2312.11805*, 2023. 3, 5
- [45] Sheng-Yu Wang, Oliver Wang, Richard Zhang, Andrew Owens, and Alexei A Efros. Cnn-generated images are surprisingly easy to spot... for now. In *ICCV*, pages 8695–8704, 2020. 3, 7, 1, 2
- [46] Zhendong Wang, Jianmin Bao, Wengang Zhou, Weilun Wang, Hezhen Hu, Hong Chen, and Houqiang Li. Dire for diffusion-generated image detection. In *ICCV*, pages 22445–22455, 2023. 3, 7, 1, 2
- [47] Siwei Wen, Junyan Ye, Peilin Feng, Hengrui Kang, Zichen Wen, Yize Chen, Jiang Wu, Wenjun Wu, Conghui He, and

- Weijia Li. Spot the fake: Large multimodal model-based synthetic image detection with artifact explanation. *NeurIPS*, 2025. 1, 2, 3, 4, 6
- [48] Chenfei Wu, Jiahao Li, Jingren Zhou, Junyang Lin, Kaiyuan Gao, Kun Yan, Sheng ming Yin, Shuai Bai, Xiao Xu, Yilei Chen, Yuxiang Chen, Zecheng Tang, Zekai Zhang, Zhengyi Wang, An Yang, Bowen Yu, Chen Cheng, Dayiheng Liu, Deqing Li, Hang Zhang, Hao Meng, Hu Wei, Jingyuan Ni, Kai Chen, Kuan Cao, Liang Peng, Lin Qu, Minggang Wu, Peng Wang, Shuting Yu, Tingkun Wen, Wensen Feng, Xiaoxiao Xu, Yi Wang, Yichang Zhang, Yongqiang Zhu, Yujia Wu, Yuxuan Cai, and Zenan Liu. Qwen-image technical report, 2025. 3, 1
- [49] Jun Xu, Tao Mei, Ting Yao, and Yong Rui. Msr-vtt: A large video description dataset for bridging video and language. In *CVPR*, 2016. 3
- [50] Shilin Yan, Ouxiang Li, Jiayin Cai, Yanbin Hao, Xiaolong Jiang, Yao Hu, and Weidi Xie. A sanity check for AI-generated image detection. In *The Thirteenth International Conference on Learning Representations*, 2025. 1, 2, 7, 8
- [51] Zhiyuan Yan, Jiangming Wang, Zhendong Wang, Peng Jin, Ke-Yue Zhang, Shen Chen, Taiping Yao, Shouhong Ding, Baoyuan Wu, and Li Yuan. Effort: Efficient orthogonal modeling for generalizable ai-generated image detection. In *ICML*, 2024. 7
- [52] An Yang, Anfeng Li, Baosong Yang, Beichen Zhang, Binyuan Hui, Bo Zheng, Bowen Yu, Chang Gao, Chengen Huang, Chenxu Lv, Chuji Zheng, Dayiheng Liu, Fan Zhou, Fei Huang, Feng Hu, Hao Ge, Haoran Wei, Huan Lin, Jialong Tang, Jian Yang, Jianhong Tu, Jianwei Zhang, Jianxin Yang, Jiayi Yang, Jing Zhou, Jingren Zhou, Junyang Lin, Kai Dang, Keqin Bao, Kexin Yang, Le Yu, Lianghao Deng, Mei Li, Mingfeng Xue, Mingze Li, Pei Zhang, Peng Wang, Qin Zhu, Rui Men, Ruize Gao, Shixuan Liu, Shuang Luo, Tianhao Li, Tianyi Tang, Wenbiao Yin, Xingzhang Ren, Xinyu Wang, Xinyu Zhang, Xuancheng Ren, Yang Fan, Yang Su, Yichang Zhang, Yinger Zhang, Yu Wan, Yuqiong Liu, Zekun Wang, Zeyu Cui, Zhenru Zhang, Zhipeng Zhou, and Zihan Qiu. Qwen3 technical report. *arXiv preprint arXiv:2505.09388*, 2025. 4
- [53] Yuan Yao, Tianyu Yu, Ao Zhang, Chongyi Wang, Junbo Cui, Hongji Zhu, Tianchi Cai, Haoyu Li, Weilin Zhao, Zhihui He, et al. Minicpm-v: A gpt-4v level mllm on your phone. *Nat Commun* 16, 5509 (2025), 2025. 5
- [54] Junyan Ye, Baichuan Zhou, Zilong Huang, Junan Zhang, Tianyi Bai, Hengrui Kang, Jun He, Honglin Lin, Zihao Wang, Tong Wu, et al. Loki: A comprehensive synthetic data detection benchmark using large multimodal models. *ICLR*, 2025. 1, 2, 3, 4
- [55] Tianyu Yu, Zefan Wang, Chongyi Wang, Fuwei Huang, Wenshuo Ma, Zhihui He, Tianchi Cai, Weize Chen, Yuxiang Huang, Yuanqian Zhao, Bokai Xu, Junbo Cui, Yingjing Xu, Liqing Ruan, Luoyuan Zhang, Hanyu Liu, Jingkun Tang, Hongyuan Liu, Qining Guo, Wenhao Hu, Bingxiang He, Jie Zhou, Jie Cai, Ji Qi, Zonghao Guo, Chi Chen, Guoyang Zeng, Yuxuan Li, Ganqu Cui, Ning Ding, Xu Han, Yuan Yao, Zhiyuan Liu, and Maosong Sun. Minicpm-v 4.5: Cooking efficient mllms via architecture, data, and training recipe, 2025. 5
- [56] Lingzhi Zhang, Zhengjie Xu, Connelly Barnes, Yuqian Zhou, Qing Liu, He Zhang, Sohrab Amirghodsi, Zhe Lin, Eli Shechtman, and Jianbo Shi. Perceptual artifacts localization for image synthesis tasks. In *ICCV*, pages 7579–7590, 2023. 1
- [57] Tianyi Zhang, Varsha Kishore, Felix Wu, Kilian Q. Weinberger, and Yoav Artzi. Bertscore: Evaluating text generation with bert. In *International Conference on Learning Representations*, 2020. 5
- [58] Lianmin Zheng, Wei-Lin Chiang, Ying Sheng, Siyuan Zhuang, Zhanghao Wu, Yonghao Zhuang, Zi Lin, Zhuohan Li, Dacheng Li, Eric Xing, et al. Judging llm-as-a-judge with mt-bench and chatbot arena. *Advances in Neural Information Processing Systems*, 36:46595–46623, 2023. 5
- [59] Nan Zhong, Yiran Xu, Sheng Li, Zhenxing Qian, and Xinpeng Zhang. Patchcraft: Exploring texture patch for efficient ai-generated image detection. *arXiv preprint arXiv:2311.12397*, 2023. 1, 2, 7
- [60] Jun-Yan Zhu, Taesung Park, Phillip Isola, and Alexei A Efros. Unpaired image-to-image translation using cycle-consistent adversarial networks. In *Proceedings of the IEEE international conference on computer vision*, pages 2223–2232, 2017. 1
- [61] Mingjian Zhu, Hanqing Chen, Mouxiao Huang, Wei Li, Hailin Hu, Jie Hu, and Yunhe Wang. Gendet: Towards good generalizations for ai-generated image detection. *arXiv preprint arXiv:2312.08880*, 2023. 7, 2
- [62] Mingjian Zhu, Hanqing Chen, Qiangyu Yan, Xudong Huang, Guanyu Lin, Wei Li, Zhijun Tu, Hailin Hu, Jie Hu, and Yunhe Wang. Genimage: a million-scale benchmark for detecting ai-generated image. In *NeurIPS*, Red Hook, NY, USA, 2023. Curran Associates Inc. 3, 7, 1, 2

# Ivy-Fake: A Unified Explainable Framework and Benchmark for Image and Video AIGC Detection

## Supplementary Material

### 6. Author and Affiliation List

**PI<sup>3</sup> Lab** Changjiang Jiang\*, Wenhui Dong\*✉, Zhonghao Zhang

**Wuhan University** Changjiang Jiang\*, Fengchang Yu

**Nanjing University** Chenyang Si, Caifeng Shan

**Stanford University** Wei Peng

**Nankai University** Xinbin Yuan

**Georgia Institute of Technology** Yifei Bi

**Jilin University** Ming Zhao

**Zhejiang University** Zian Zhou

\* Equal contribution. ✉ Corresponding author.

### 7. License

For all datasets in our experiments and datasets, FLUX.1 [27] and Lora Flux [27] falls under the FLUX.1 [dev] Non-Commercial License. WildFake [23] is released under an open-source license, making it freely available for research and non-commercial use; Qwen-Image [48] is licensed under Apache 2.0; Sora [9] is a commercial, non-open-source text-to-video model provided via ChatGPT Plus/Pro; user-generated content is owned by the user and allows (subject to usage policies) non-commercial use, but the model itself is closed-source.

Stable Diffusion [6], while originally open-source under Creative ML OpenRAIL-M (e.g., versions 1.X, 2.1, SDXL), has transitioned in newer versions (SD3.x, SD3.5) to the Stability AI Community License, which permits free use for individuals or entities with annual revenue under USD 1 million, but requires a paid Enterprise License for larger-scale or commercial usage.

During Ivy-Fake construction and experimentation, we accessed Gemini API and ChatGPT API to ensure annotation and evaluation’s quality and reproducibility. We explicitly state that all data generated using these commercial APIs are used solely for academic research and non-commercial purposes, fully complying with the respective API usage agreements and ethical guidelines. No Gemini- or ChatGPT-derived content is redistributed for any commercial training, deployment, or monetization purposes.

### 8. Related Work

#### 8.1. Methods for Synthetic Content Detection

Due to growing concerns about the misuse of synthetic data [15], research on AI-generated content (AIGC) detec-

tion has expanded rapidly in recent years. Most existing models for AI-generated images and videos formulate the task as binary classification, simply predicting whether the content is "real" or "fake." Representative examples include CNN-based AIGVDet [2], CNNSpot [45] and Transformer-based models such as DIRE [46] and AIDE [50]. Meanwhile, several works have explored the application of multimodal large language models (MLLMs) to AIGC detection, including Synartifact [10] and Bi-LORA [26]. However, these approaches largely overlook the importance of interpretability in AIGC detection.

Some efforts attempt to introduce interpretability by leveraging spatial annotations [17] or frequency-domain artifact analysis [56]. Nevertheless, the resulting explanations are often difficult for humans to comprehend, as they lack clarity in natural language. This limitation is particularly evident in the video domain, where AI-generated content frequently exhibits obvious flaws, e.g., incoherent frame transitions and object inconsistency, that are easily noticed and reasoned about by humans [15]. FakeClue [47] introduces the use of vision-language models (VLMs) to provide interpretability for image-level detection, but it does not offer a unified framework that integrates both images and videos.

#### 8.2. Datasets for Synthetic Content Detection.

Early datasets for synthetic content detection, such as CNNSpot [45], primarily collected fake images generated by GAN-based models [8, 18, 60]. However, with the advent of more advanced generative architectures like diffusion models [16, 21, 22, 33, 37] and their variants, the authenticity of generated content has significantly increased, making it more challenging for detection models to discern. This has spurred the development of newer datasets, including ArtiFact [10], GenImage [62], and WildFake [23]. GenImage [62] comprises images from the 1000 ImageNet [39] categories, generated by eight state-of-the-art generators such as Stable Diffusion [37] and Midjourney. Nevertheless, these datasets predominantly focus on image-based content. More recently, datasets emphasizing interpretability have also been introduced. FakeClue [47] contains a large amount of image data with explainability annotations but lacks video data. LOKI [54] offers data across 26 different categories and includes 18,000 distinct questions; however, its volume of multimodal data is relatively small and primarily suited for evaluation rather than comprehensive model training. Therefore, a critical gap exists for a unified

benchmark encompassing both image and video modalities to rigorously evaluate the performance of contemporary AIGC detectors.

## 9. GRPO

Following DeepSeek-R1 [19], we adapt the Group Relative Policy Optimization (GRPO) [41], an online RL algorithm designed to maximize the advantage of generated completions while constraining policy divergence from a reference model. We formalize our training process of Ivy-xDetector using GRPO below. Let  $p$  denote a sampled prompt, and let  $o_1, o_2, \dots, o_n$  be a group of completions generated by the current policy  $\pi_\theta$ . For each completion  $G_i$ , a reward  $r_i$  is computed using a rule-based reward function. The group advantage for each completion is then calculated as:

$$\hat{A}_{i,t} = \frac{r_i - \text{mean}(r)}{\text{std}(r)} \quad (1)$$

where  $\beta$  is a coefficient that balances advantage maximization and KL regularization, and the clipping operator  $\text{clip}(\dots, 1 - \epsilon, 1 + \epsilon)$  constrains the update magnitude. To regularize policy updates, we estimate the token-level Kullback-Leibler (KL) divergence between the current policy  $\pi_\theta$  and a reference policy  $\pi_{ref}$ .

**Reward Model.** For effective RL, we employ a rule-based reward that consists of accuracy and format rewards. We introduce a solid accuracy reward for AIGC Detection, which utilizes distinct functions to evaluate binary classification task. This allows for a more appropriate assessment based on the expected answer type.

- **Accuracy Reward:** The accuracy reward assigns a score of **1** if the label in `<conclusion>` exactly matches the ground-truth classification `real` and `fake` and **0** otherwise.
- **Format Reward:** The format reward assigns a score of **1** if the output strictly follows the structural requirements by enclosing the reasoning within `<think></think>` tags and the final decision within `<conclusion></conclusion>` tags, and **0** otherwise.

## 10. Effect of Incorporating Human-Annotated Labels via gemini 2.5 pro on Accuracy

To assess the impact of human-annotated labels on model performance, we compare the accuracy of final conclusion predictions under two settings: (i) with labels incorporated via the `gemini 2.5 pro`, and (ii) without labels. The evaluation was conducted on about 1,000 examples from the test set.

Annotation Setting	Accuracy (Acc)
With Label	1.000
Without Label	0.785

Table 8. Accuracy of conclusion prediction with and without incorporating labels.

As shown in Table 8, incorporating ground-truth labels results in a substantial performance gain, yielding perfect accuracy (1.000), compared to 0.785 without labels. The drastic performance gap suggests potential limitations in label-free or weakly supervised setups when applied to tasks requiring fine-grained semantic understanding.

## 11. Data Distribution

### 12. Additional Experiment

#### 12.1. Synthetic Image Detection

We evaluated our AIGC detector on the GenImage [62] and Chameleon [50] benchmarks.

As shown in Table 5, GenImage comprises seven subsets generated by leading models, i.e., Midjourney, Stable Diffusion v1.4 & v1.5, ADM, GLIDE, Wukong, VQDM, and BigGAN. We compared against five state-of-the-art detectors, which are CNNSpot [45], F3Net [34], DIRE [46], GenDet [61], PatchCraft [59], and AIDE [50].

Notably, our detector surpasses previous state-of-the-art methods such as AIDE (86.88%) and PatchCraft (82.30%) by a large margin, even though it is trained under a unified multimodal paradigm rather than a generator-specific setting. The improvement is especially pronounced on challenging generators like *ADM*, *GLIDE*, and *BigGAN*, where conventional CNN- or patch-based detectors often fail to capture high-frequency inconsistencies or generalized texture patterns.

**Notably, our model is trained with only 130K image samples—fewer than GenImage’s 2M+ training images—yet still achieves superior generalization performance.**

#### 12.2. Synthetic Video Detection

As shown in Table 6, we evaluate the performance of our detector on the GenVideo benchmark [12].

Specifically, Ivy-xDetector achieves an average F1 score of **95.26%** and recall of **95.28%**, substantially surpassing the prior state-of-the-art DeMamba (F1 = 90.20%). The improvement is particularly evident on challenging categories such as *HotShot*, *Lavie*, and *Show-1*, where previous methods tend to overfit to specific generative distributions or temporal artifacts. Our results indicate that the unified MLLM-based detection paradigm not only captures spa-

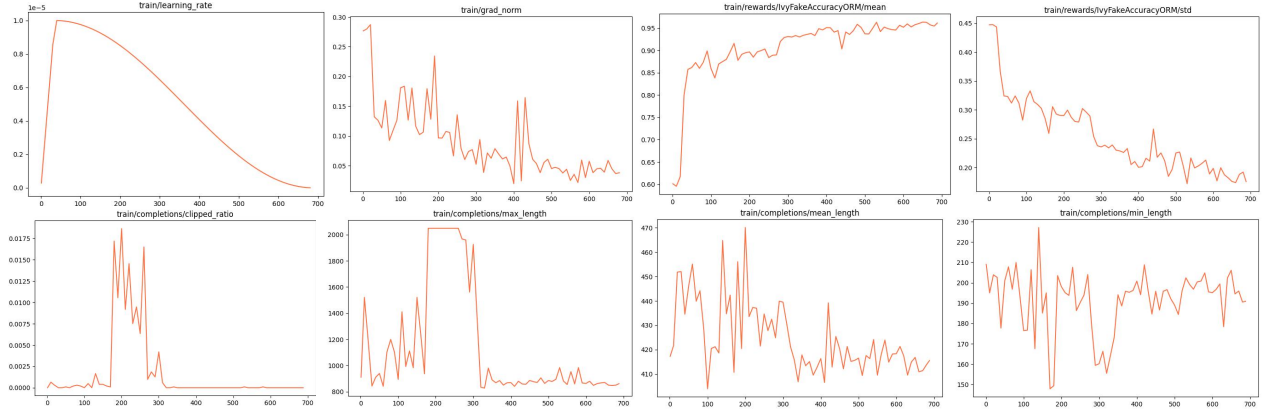


Figure 6. Final Reinforcement Learning Training Curves.

$$\mathcal{L}_{\text{GRPO}}(\theta) = -\frac{1}{K} \sum_{k=1}^K A^{(k)} \ell^{(k)}(\theta) + \beta \text{KL}(\pi_{\theta}(\cdot|x) \parallel \pi_{\text{ref}}(\cdot|x)). \quad (2)$$

tial inconsistencies but also learns transferable temporal-spatial representations, leading to more robust generalization across unseen generative models.

**Notably, our model is trained with only 64K video samples—over 35× fewer than DeMamba’s 2.295M training videos—yet still achieves superior generalization performance.**

### 13. Prompts

Here we provide the prompts that are mainly used in this study. The default system prompt can be seen in Figure 11. As illustrated by the following figures, there are five distillation prompts we used in this paper that mainly can be divided into the following three parts:

**Prompt Template for Image Data Distillation:** Since image data consists of a single frame, it can be treated as a static instance. Therefore, AIGC detection mainly focuses on identifying spatial anomalies. Detail prompt can be found in Figure 7 and 9.

**Prompt Template for Video Data Distillation:** Compared to images, video inputs provide continuous multi-frame context. This allows for detection along both spatial and temporal anomaly dimensions. Detail prompt can be found in Figure 8 and Figure 10.

**GPT Assisted Evaluation Prompt:** To assess the quality of model outputs, we design a GPT-based evaluator prompt that scores responses across four dimensions: Completeness, Relevance, Level of Detail, and Explanation. The evaluator receives a structured pair of GroundTruth and ModelOutput, each containing a <think> section (reasoning) and a <conclusion> (final judgment). The model must return a structured JSON object with integer scores

(1–5) for each dimension. The prompt is provided in Figure 12.

### 14. Training Detail

The RL training process of Ivy-xDetector is illustrated in Fig. 6. Our GRPO training exhibits a stable increase in reward, eventually reaching 0.95. However, we also observe that both the clip ratio and the maximum response length surge sharply around 200–300 steps, suggesting that a portion of the training samples may be overly challenging for the model.

### 15. Case Study: Qualitative Comparison of Methods

According to Figures 13, 14, 15, and 16, Ivy-xDetector consistently demonstrates superior performance in detecting both spatial and temporal anomalies, providing stronger generalization and robustness compared to existing baselines.

$$\mathbb{D}_{\text{KL}}[\pi_{\theta} \parallel \pi_{\text{ref}}] = \frac{\pi_{\text{ref}}(o_{i,t} \mid p, o_{i,<t})}{\pi_{\theta}(o_{i,t} \mid p, o_{i,<t})} - \log \frac{\pi_{\text{ref}}(o_{i,t} \mid p, o_{i,<t})}{\pi_{\theta}(o_{i,t} \mid p, o_{i,<t})} - 1. \quad (3)$$

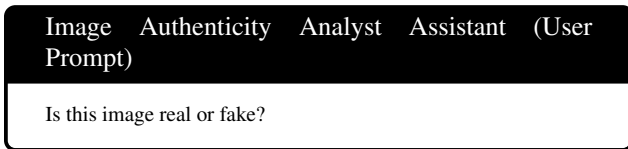


Figure 7. User Prompt Template for Image Data Distillation

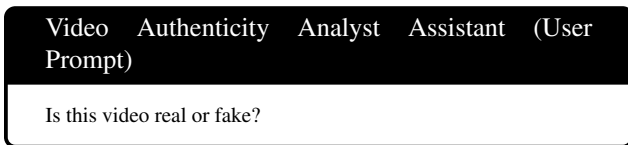


Figure 8. User Prompt Template for Video Data Distillation

## Image Authenticity Analyst Assistant (System Prompt)

### ## Role

Expert AI system for detecting image by analyzing visual anomalies across **spatial plausibility**.

### ## Analysis Dimensions

#### ### Spatial Features: static anomaly detection

##### - **Impractical Luminosity**

- Scene brightness measurement
- Invisible light source detection (physical validation)

##### - **Localized Blur**

- Focus distribution mapping (sharpness gradient)
- Artificial depth-of-field identification (algorithmic artifacts)

##### - **Illegible Letters**

- OCR text extraction
- Character structural integrity (stroke continuity)

##### - **Distorted Components**

- Anatomical/proportional accuracy (biological/object logic)
- Physics compliance (material/gravity validation)

##### - **Omitted Components**

- Object completeness check (edge/detail absence)
- Partial rendering artifact detection (AI-generated traces)

##### - **Spatial Relationships**

- Contextual object placement (scene plausibility)
- Perspective consistency (geometric projection)

##### - **Chromatic Irregularity**

- Color database comparison (natural distribution)
- Unnatural hue detection (oversaturation/abrupt gradients)

##### - **Abnormal Texture**

- Surface pattern regularity (texture repetition)
- Material property coherence (reflectance/roughness validation)

### ## Reasoning Step

#### 1. **Spatial Analysis**

- Analyze static features (e.g., lighting, text, objects)

#### 2. **Conclusion:** Only real or fake.

- real: Contains verifiable capture device signatures and natural physical imperfections.
- fake: Exhibits synthetic fingerprints including but not limited to over-regularized textures and non-physical light interactions.

The assistant first thinks about the reasoning step in the mind and then provides the user with the reason. The reasoning step and conclusion are enclosed within `<think>` `</think>` and `<conclusion>` `</conclusion>` tags, respectively, i.e., `<think>` reasoning step here `</think>` `<conclusion>` real or fake `</conclusion>`. `<conclusion>` content must strictly align with the user-provided authenticity label (real/fake) in both value and semantic context.

Figure 9. System Prompt Template for Image Data Distillation

## Video Authenticity Analyst Assistant (System Prompt)

### ## Role

Expert AI system for detecting videos by analyzing visual anomalies across **temporal coherence** (inter-frame dynamics) and **spatial plausibility** (intra-frame logic).

### ## Analysis Dimensions

#### ### 1. Temporal Features: Multi-frame dynamic anomaly detection - **Luminance Discrepancy**

- Shadow direction consistency (cross-frame comparison)
- Light source coordination (temporal validation)
- **Awkward Facial Expression**
  - Facial muscle motion continuity (expression dynamics)
  - Emotion-context alignment (temporal coherence)
- **Duplicated Components**
  - Repeating element pattern recognition (cross-frame tracking)
  - Natural variation analysis (sequence validation)
- **Non-Spatial Relationships**
  - Object interaction physics (motion trajectory validation)
  - Fusion/penetration anomalies (temporal detection)

#### ### 2. Spatial Features: Single-frame static anomaly detection

- **Impractical Luminosity**
  - Scene brightness measurement (single-frame analysis)
  - Invisible light source detection (physical validation)
- **Localized Blur**
  - Focus distribution mapping (sharpness gradient)
  - Artificial depth-of-field identification (algorithmic artifacts)
- **Illegible Letters**
  - OCR text extraction (single-frame recognition)
  - Character structural integrity (stroke continuity)
- **Distorted Components**
  - Anatomical/proportional accuracy (biological/object logic)
  - Physics compliance (material/gravity validation)
- **Omitted Components**
  - Object completeness check (edge/detail absence)
  - Partial rendering artifact detection (AI-generated traces)
- **Spatial Relationships**
  - Contextual object placement (scene plausibility)
  - Perspective consistency (geometric projection)
- **Chromatic Irregularity**
  - Color database comparison (natural distribution)
  - Unnatural hue detection (oversaturation/abrupt gradients)
- **Abnormal Texture**
  - Surface pattern regularity (texture repetition)
  - Material property coherence (reflectance/roughness validation)

### ## Reasoning Step

#### 1. **Temporal Analysis**

- Track dynamic features across frames (e.g., shadows, expressions)

#### 2. **Spatial Analysis**

- Analyze static features per frame (e.g., lighting, text, objects)

#### 3. **Conclusion:** Only real or fake.

- real: Contains verifiable capture device signatures and natural physical imperfections.
- fake: Exhibits synthetic fingerprints including but not limited to over-regularized textures and non-physical light interactions.

The assistant first thinks about the reasoning step in the mind and then provides the user with the reason. The reasoning step and conclusion are enclosed within `<think>` `</think>` and `<conclusion>` `</conclusion>` tags, respectively, i.e., `<think>` reasoning step here `</think>` `<conclusion>` real or fake `</conclusion>`. `<conclusion>` content must strictly align with the user-provided authenticity label (real/fake) in both value and semantic context.

Figure 10. System Prompt Template for Video Data Distillation

## Default System Prompt

You are an AI-generated content detector. Given a single media (image or video), classify it as real or fake. Provide detailed reasoning inside the `<think>...</think>` tags, including your step-by-step thought process.

Your output must begin with `<think>` and end with `</conclusion>`.

Then output exactly one word in lowercase—either real or fake—wrapped in `<conclusion>...</conclusion>`.

Do not include any other words. If uncertain, choose the most likely class.

Figure 11. Default System Prompt for Training and Evaluation

## GPT Assisted Evaluation Prompt

### ## Role

You are an impartial evaluator. Your task is to assess whether a model-generated response accurately and coherently matches a human-annotated reference answer.

Each input contains two structured components:

- `think`: the reasoning or analytical explanation
- `conclusion`: the final judgment (e.g., real or fake)

### ## Evaluation Dimensions

You should compare the **ModelOutput** to the **GroundTruth**, and assign integer scores from 1 to 5 (no decimals) for the following four dimensions:

#### 1. Completeness

- Does the ModelOutput address all aspects covered in the GroundTruth?
- More complete responses should include all relevant information, especially key golden clues.
- Incomplete or partially aligned answers should receive lower scores.

#### 2. Relevance

- Does the ModelOutput discuss the same detection dimensions as in the GroundTruth?
- Temporal features include:
  - Luminance discrepancy
  - Duplicated components
  - Awkward facial expressions
  - Motion inconsistency
- Spatial features include:
  - Abnormal texture
  - Distorted or omitted components
  - Chromatic irregularity
  - Impractical luminosity
  - Localized blur, etc.
- Penalize if irrelevant aspects are introduced or relevant ones are missing.

#### 3. Level of Detail

- Does the ModelOutput describe fine-grained visual cues in each dimension?
- High scores require specific subcomponent elaboration, not just general terms.
- Penalize vague or generic responses that lack specific observations.

#### 4. Explanation

- Is the reasoning in `<think>` logically consistent with the `<conclusion>`?
- The explanation should provide clear, causally-linked justifications.
- Penalize if the conclusion contradicts the reasoning or lacks support.

Figure 12. GPT Assisted Evaluation Prompt

	    	Conclusion Validity
 <b>Ivy-xDetector</b>	<p>&lt;think&gt;1. <b>Spatial Analysis</b>: The lighting, ... <i>expected from real materials</i>. The image is <i>uniformly sharp</i> ... seem generally correct, but the <i>perfection of forms</i> (e.g., identical wine bottles, perfectly aligned shelves) leans towards artificiality ... appear geometrically sound and plausible for an interior design concept ... <i>lacking the unique variations</i> found in natural wood. 2. <b>Conclusion</b>: The image <i>exhibits synthetic fingerprints</i> ... lacking the imperfections and variations inherent in real-world photography.&lt;/think&gt;</p>	<b>Conclusion</b> <i>fake</i> 
 <b>GPT-4o</b>	<p>&lt;think&gt;Upon analyzing the image of the interior space: 1. <b>Illumination Inconsistency</b>: The lighting appears consistent ... <i>light directions are evident</i>. 2. <b>Unnatural Content Placement</b>: Furniture placement ... dining table, and seating. 3. <b>Unrealistic Physical Properties</b>: Material properties ... object interactions or physical impossibilities. 4. <b>Digital Manipulation Signatures</b>: Edges are ... <i>with the intended function</i>. <b>Overall</b>: there <i>are no signs of anomalies</i> ... appears to capture a <i>real</i>.&lt;/think&gt;</p>	<b>Conclusion</b> <i>real</i> 
 <b>Gemini-2.5</b>	<p>&lt;think&gt;The image displays <i>consistent lighting and natural shadows</i> ... without signs of partial rendering. The spatial relationships between objects and the perspective are consistent with ... <i>indicative of repetitive patterns found in synthetic images</i>. Based on the absence ... generated imagery, the image appears to be a <i>real</i> photograph.&lt;/think&gt;</p>	<b>Conclusion</b> <i>real</i> 
 <b>InternVL3-8B</b>	<p>&lt;think&gt;The image appears to be a modern, well-lit room with a sleek design. <b>Impractical Luminosity</b>: The lighting seems evenly distributed, but there's no visible light source ... <i>have concealed lighting</i>. <b>Localized Blur</b>: The image is sharp throughout, with no noticeable blur, suggesting high-quality rendering. ... <b>Abnormal Texture</b>: The textures ... seems to have high-quality, realistic features <i>without obvious anomalies</i>.&lt;/think&gt;</p>	<b>Conclusion</b> <i>real</i> 
 <b>Qwen2.5-VL-7B</b>	<p>&lt;think&gt;Let's analyze the image step by step: <b>Impractical Luminosity</b>: The lighting appears consistent and well-distributed across the room ... <b>Spatial Relationships</b>: - The placement of objects like the wine rack, table, chairs, and <i>sofa is logical and follows typical spatial relationships</i> found in a living space ... that would suggest the <i>image is real</i>. The image appears to be a real photograph of a well-designed interior space.&lt;/think&gt;</p>	<b>Conclusion</b> <i>real</i> 

Figure 13. **Image example 1** where **Ivy-xDetector** successfully detects subtle spatial anomalies missed by baselines.

	  	Conclusion Validity
 Ivy-xDetector	<p>&lt;think&gt;1. <b>Spatial Analysis</b>: ... the transition between the sharp foreground (tiger) and the blurred background <i>isn't perfectly natural</i>, particularly around the fur edges. ... <b>Spatial Relationships</b>:... The texture of the tiger's fur, especially on the back and shoulder, appears overly smooth and lacks the fine, distinct detail expected in high-resolution photography. Similarly, the snow texture looks somewhat uniform and <i>lacks the complex, random variations</i> of real snow. ... 2. <b>Conclusion</b>: The image exhibits <i>synthetic fingerprints</i>, which <i>lack natural complexity and detail</i>, appearing overly smooth and regularized.</p>	<b>Conclusion</b> fake ✓
 GPT-4o	<p>&lt;think&gt;1. <b>Illumination Inconsistency</b>: The lighting appears <i>coherent</i> across the tiger and the snow. Shadows align properly with a consistent light source direction. 2. <b>Facial Feature Anomalies</b>: The tiger's features ... <i>appear natural and well-integrated</i>. ... 4. <b>Unrealistic Physical Properties</b>: The interaction between the tiger's paws and the snow appears convincing with visible snow compression. ... 6. <b>Semiotic Plausibility</b>: The scene is <i>semantically coherent</i>—a tiger in a snowy environment reflects natural habitat possibilities. ... the image <i>does not exhibit significant anomalies</i> associated with synthetic generation or manipulations.&lt;/think&gt;</p>	<b>Conclusion</b> real ✗
 Gemini-2.5	<p>&lt;think&gt;1. <b>Spatial Analysis</b>: The lighting <i>seems consistent with natural light sources</i> (sunlight) casting shadows and highlights on the tiger and snow. No abrupt or unnatural blur regions are detected. ... <b>Omitted Components</b>: The tiger is depicted completely within the image. <i>No signs of missing details or partial rendering artifacts</i> are apparent. ... <b>Spatial Relationships</b>: The tiger is situated in a snowy environment, which is a plausible habitat for some tiger subspecies. ... <b>Chromatic Irregularity</b>: The colors of the tiger's fur, eyes, mouth, and the surrounding snow and background exhibit natural hues ... <i>No unnatural saturation or gradients</i> are detected. <b>Abnormal Texture</b>: The textures of the tiger's fur and the snow appear detailed and <i>naturally irregular</i> ... with a real photograph and shows <i>no significant spatial anomalies</i> that would indicate it is fake.&lt;/think&gt;</p>	<b>Conclusion</b> real ✗
 InternVL3-8B	<p>&lt;think&gt;Let's analyze the spatial features: 1. <b>Impractical Luminosity</b>: The lighting <i>appears natural</i>, with no obvious signs of an invisible light source. ... 4. <b>Spatial Relationships</b>: The tiger's position in the snow and the background context <i>seem plausible</i>. 5. <b>Chromatic Irregularity</b>: The <i>colors are natural</i>, with no unnatural hues or saturation. 6. <b>Abnormal Texture</b>: The snow and tiger's fur textures appear realistic. Considering these factors, the image seems to have <i>natural features</i> without obvious synthetic artifacts.&lt;/think&gt;</p>	<b>Conclusion</b> real ✗
 Qwen2.5-VL-7B	<p>&lt;think&gt;To determine if the image is real or fake, we need to analyze various spatial features: 1. <b>Impractical Luminosity</b>: There's no visible light source that would explain the brightness, suggesting it ... like a zoo or wildlife sanctuary. 2. <b>Localized Blur</b>: The tiger's fur and facial features appear sharp ... 6. <b>Spatial Relationships</b>: ...with <i>no unusual perspective or positioning</i> ... There are <i>no unnatural hues or color gradients</i>. 8. <b>Abnormal Texture</b>: The texture of the tiger's fur and the snow appears natural and consistent with real-life observations. ... It appears to be a <i>real photograph</i> of a tiger in a snowy environment.&lt;/think&gt;</p>	<b>Conclusion</b> real ✗

Figure 14. Image example 2 illustrating improved robustness of Ivy-xDetector against visually deceptive artifacts.

		<b>Conclusion Validity</b>
 Ivy-xDetector	<p>&lt;think&gt;1. <b>Temporal Analysis</b>: ... the interaction between the person in the blue shirt and the beige chair. The trajectory ... by a person. The way ... without proper support or effort from the person suggests manipulation. 2. <b>Spatial Analysis</b>: While the overall scene ... the chair's motion overrides most spatial plausibility checks. No specific ... but the unnatural movement highlights the artificiality of the interaction. 3. <b>Conclusion</b>: The video exhibits synthetic fingerprints, ... , indicating manipulation.&lt;/think&gt;</p>	<b>Conclusion</b> <i>fake</i> 
 GPT-4o	<p>&lt;think&gt;<b>Temporal Features</b>: sand and objects looks ... natural. <b>Spatial Features</b>: The chair exhibits ... no evidence of visual anomalies, ... properties ... for the environment. ...The physical interactions, ... with a genuine scenario.&lt;/think&gt;</p>	<b>Conclusion</b> <i>real</i> 
 Gemini-2.5	<p>&lt;think&gt;The video shows ... spatial anomalies. <b>Temporal Analysis</b>: The shadows and lighting seem consistent across the frames as people move and interact with the chair ... follow expected physics. <b>Spatial Analysis</b>: Lighting is consistent with a single, natural light source ... without over-regularization. .... the video appears consistent with a real recording.&lt;/think&gt;</p>	<b>Conclusion</b> <i>real</i> 
 InternVL3-8B	<p>&lt;think&gt;Okay, let's analyze this video frame ... it's real or fake. First, I'll look ... no signs of awkwardness or discontinuity. Next, I'll examine the spatial features. The scene is set in ... no obvious signs of unnatural blur, chromatic irregularities, or distorted components that would indicate digital manipulation. Considering both temporal and spatial analysis, the video doesn't exhibit any clear signs of temporal or spatial anomalies. The actions, lighting, and object placements ... video appears to be authentic.&lt;/think&gt;</p>	<b>Conclusion</b> <i>real</i> 
 Qwen2.5-VL-7B	<p>&lt;think&gt; ... spatial features. <b>Temporal Analysis</b>: The shadows cast by the chair and the person appear ... that the lighting is natural and not artificially manipulated. The interaction between the person and the chair ... is a logical action given the context. <b>Spatial Analysis</b>: The scene appears well-lit ... focus is sharp ... colors are natural and there are no unnatural hues. The sand and the chair looks realistic and there are no irregularities ... no signs of artificial manipulation or synthetic fingerprints.&lt;/think&gt;</p>	<b>Conclusion</b> <i>real</i> 

Figure 15. Video example 1 showcasing Ivy-xDetector’s superior ability to detect subtle cross-frame temporal artifacts.

		<b>Conclusion Validity</b>
 Ivy-xDetector	<p>&lt;think&gt;1. <b>Temporal Analysis</b>: <b>Luminance Discrepancy</b>: The lighting appears consistent across the scene ... are not discernible for analysis. 2. <b>Spatial Analysis</b>: <b>Impractical Luminosity</b>: The overall brightness of the scene is plausible for a sunny day ... <b>Spatial Relationships</b>: The placement of buildings, people ... perspective seems generally consistent. <b>Abnormal Texture</b>: This is the most notable area. The texture of the stone walls, particularly on the right-hand structure ... <b>lacking the intricate detail of real waves and ripples under sunlight</b>. 3. <b>Conclusion</b>: The video exhibits <b>synthetic fingerprints</b>, primarily identified through spatial analysis. The textures, especially on the stone structures, <b>lack the natural complexity and variation</b> expected in real-world materials, which is characteristic of AI-generated content.&lt;/think&gt;</p>	<b>Conclusion</b> <b>fake</b> 
 GPT-4o	<p>&lt;think&gt;To determine ... both temporal and spatial features: 1. <b>Temporal Analysis</b>: The movement of the water shows natural fluid dynamics ... people move naturally across the frames. The human motions (walking, gathering, posture changes) <b>are smooth and align with physical plausibility</b>. 2. <b>Spatial Analysis</b>: The architectural elements ... <b>no signs of over-regularized patterns</b> or artifacts are detected. The sea exhibits natural interaction with the rocks ... Details such as human attire, proportions, and gestures appear accurate and vary naturally. Both temporal coherence and spatial plausibility align with the characteristics of a real scene. <b>No signs of AI-generation artifacts</b>.&lt;/think&gt;</p>	<b>Conclusion</b> <b>real</b> 
 Gemini-2.5	<p>&lt;think&gt;I will analyze both temporal and spatial features for potential anomalies. <b>Temporal Analysis</b>: People are <b>moving naturally</b> across the plaza and stairs. Their motion appears continuous and realistic frame-to-frame. ... <b>No impractical luminosity</b> is detected. The scene's focus seems uniform and natural; no localized blurring or artificial depth of field is apparent ... Spatial relationships between elements (buildings relative to cliff and plaza, rocks in the sea) are <b>logical and adhere to perspective rules</b>. There are no detectable temporal coherence ... with <b>synthetic media</b> in these frames.&lt;/think&gt;</p>	<b>Conclusion</b> <b>real</b> 
 InternVL3-8B	<p>&lt;think&gt;Upon analyzing the video, I observe the following key points: 1. <b>Temporal Features</b>: The shadows and lighting appear consistent across frames, <b>indicating natural lighting conditions</b> ... <b>Non-Spatial Relationships</b>: The objects and people move naturally, with no unnatural interactions. 2. <b>Spatial Features</b>: The scene lighting <b>is consistent with natural daylight</b>. ... <b>Spatial Relationships</b>: The placement of objects and people <b>is contextually appropriate</b>. <b>Abnormal Texture</b>: The textures of the buildings and natural elements <b>look realistic</b>. Given these observations, the video does not exhibit any obvious signs of manipulation or synthetic generation. The elements within the frames align with what one would <b>expect in a real-world</b> setting.&lt;/think&gt;</p>	<b>Conclusion</b> <b>real</b> 
 Qwen2.5-VL-7B	<p>&lt;think&gt;To determine if the video is real or fake, we need to analyze it using the provided dimensions of temporal and spatial features. <b>Temporal Analysis</b>:... <b>indicate a real video</b> ... do not <b>show any repeating patterns</b>... The objects ... interact naturally ... <b>Spatial Analysis</b>: The scene appears well-lit with natural sunlight, which is consistent with an outdoor setting. There are <b>no signs of artificial lighting</b> that would be inconsistent with the environment. ... <b>Abnormal Texture</b>: The textures of the buildings and the sea appear natural and coherent. ... that would suggest the video is fake. The video appears to be <b>a genuine capture</b> of a real location.&lt;/think&gt;</p>	<b>Conclusion</b> <b>real</b> 

Figure 16. Video example 2 showcasing Ivy-xDetector’s superior ability to detect subtle cross-frame temporal artifacts.